

UCSF

UC San Francisco Electronic Theses and Dissertations

Title

The Impact of Proteoglycan Degradation and Fragmentation on T1rho Relaxation Times

Permalink

<https://escholarship.org/uc/item/7rz1m418>

Author

Veres, Joanna

Publication Date

2024

Peer reviewed|Thesis/dissertation

The Impact of Proteoglycan Degradation and Fragmentation on T1rho Relaxation Times

by
Joanna Veres

THESIS
Submitted in partial satisfaction of the requirements for degree of
MASTER OF SCIENCE

in
Biomedical Imaging

in the
GRADUATE DIVISION
of the
UNIVERSITY OF CALIFORNIA, SAN FRANCISCO

Approved:

DocuSigned by:
Aaron Fields Aaron Fields
DECFACABA5674BF... Chair

DocuSigned by:
Galateia Kazakia Galateia Kazakia

Signed by:
Daehyun Yoon Daehyun Yoon

DocuSigned by:
Peder Larson Peder Larson
1644A2CD853841E...

Committee Members

Dedication and Acknowledgement

I would like to sincerely thank everyone in the Field's lab for their constant support, advice, and knowledge throughout this project. I could not have done this work without their technical expertise and gracious help, and am exceptionally grateful.

To my biggest supporters and favorite people, my amazing mom and sister, I cannot properly express my deepest appreciation for the lifelong love and encouragement they have always given me. Without them as my personal cheerleaders, I never would have had the strength to reach for my dreams.

The Impact of Proteoglycan Degradation and Fragmentation on T1rho Relaxation Times

Joanna Veres

Abstract

266 million individuals are diagnosed with intervertebral disc degeneration annually. Most of these individuals experience pain and reduced mobility, but some are asymptomatic. In contrast to age-related physiologic disc degeneration, pathologic disc degeneration is hypothesized to entail changes to the proteoglycan matrix within the disc. T1rho-weighted MR imaging has the ability to detect subtle changes in disc biochemistry, and may therefore discriminate between pathologic vs. physiologic disc degeneration. However, the contribution of individual biochemical changes to T1rho signals is unclear. Therefore, the goal of this study is to elucidate the individual roles of proteoglycan concentration and molecular weight on T1rho relaxation time. To do this, MRI phantoms with prescribed differences in the concentration and molecular weight of proteoglycan-mimicking dextrans were fabricated and imaged with T1rho-weighted MRI. Results showed that changing the dextran concentration changed T1rho relaxation times by up to 8 percent, while varying dextran size changed T1rho relaxation times by up to 47 percent. Proteoglycan fragmentation is an early marker of disc degeneration that precedes proteoglycan loss from the disc. Prior studies reported that T1rho relaxation times are correlated with disc proteoglycan content. Thus, our findings are important because they are the first to show that T1rho relaxation times are also sensitive to polysaccharide fragment size, and therefore T1rho relaxation times in the disc may reflect proteoglycan degradation in the very early stages of disc degeneration.

Contents

1	Introduction	1
2	Methods	2
2.1	Phantoms with Single Dextran Size	2
2.2	Phantoms with Sonicated Dextran	2
2.3	T1rho/T2 Weighted MRI Sequence	4
2.4	Images Processing	4
2.5	Data Analysis	5
3	Results	5
3.1	Phantoms with Single Dextran Size	5
3.2	Phantoms with Sonicated Dextran	7
4	Discussion	7
5	Conclusion	10

List of Figures

1	A Healthy Intervertebral Disc	1
2	Dextran Agarose Phantom	3
3	Custom Foam Phantom Holder	4
4	Dicom Processing Pipeline	5
5	Single Molecular Weight Phantom T1rho Across Concentrations and Molecular Weights .	6
6	T1rho Relaxation Vs Sonication Time	7
7	T1rho Relaxation Vs Molecular Weight	8
8	Sonicated Dextran Phantom T1rho Relaxation vs Interpolated Molecular Weight With Known Molecular Weight Phantoms	9
9	Sonication Phantom Data and Bovine Degeneration Model Comparison	10

List of Tables

1 Dextran Concentrations and Molecular Weight for Single Molecular Weight Phantoms	3
2 Mean T1rho Relaxation Time for Single Molecular Weight Phantoms with One Way ANOVA. . .	5

1 Introduction

The intervertebral discs (IVDs) are soft tissues located between vertebrae that confer spinal flexibility, distribute mechanical loads, and dissipate energy. The disc consists of two main parts, the nucleus pulposus (NP) and annulus fibrosus (AF)(**Fig. 1**)[1]. The NP is a central, gelatinous tissue composed of cells populating a collagen and proteoglycan-rich matrix that undergoes changes in water content in response to diurnal loading patterns [2]. The AF is a series of concentric lamellae containing parallel collagen fiber bundles and elastin fibers that restrict the deformation of the NP[2].

Disc degeneration is an age-related process characterized by biochemical and structural changes that often cause pain, limit mobility, and negatively impact a patient’s quality-of-life [3]. Given that approximately 4 in 10 adults over age 40 and 8 in 10 people over 80 have some degree of disc degeneration, better understanding the physiologic changes caused by disc degeneration is very important [4].

While disc degeneration commonly associates with chronic low back pain (cLBP), many instances of disc degeneration are asymptomatic. There is evidence to suggest that the certain biomarkers can differentiate pathologic from physiologic disc degeneration [5].

Aggrecan fragmentation and depletion is one of the most significant biochemical changes that occurs with degeneration because aggrecan is the most abundant proteoglycan in the NP [6]. During disc degeneration, aggrecanase activity (primarily ADAMTS-4 and -5) generates one smaller, hyaluronic acid bound fragment and one larger unbound fragment that can freely diffuse throughout the disc. These unbound fragments are trapped in the NP by the dense cartilage endplate matrix and accumulate. Overtime, with continued proteolysis, the unbound fragments increasingly become smaller and eventually are lost from the disc [7].

These proteoglycan changes can be measured in vivo using T1rho MRI. T1rho MRI measures low-frequency macromolecule interactions because of a secondary “spin lock” pulse following the initial 90 degree pulse [8]. Prior studies showed that lower T1rho relaxation times associate with lower sGAG content in the disc [9]. However, because prior studies only measured the total amount of proteoglycans

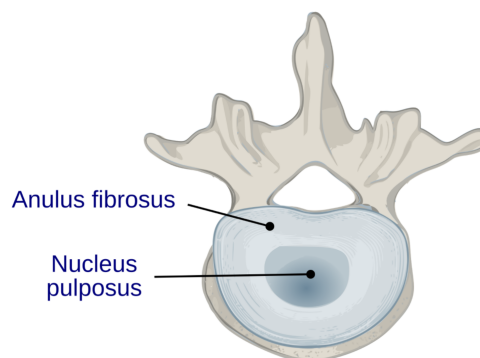


Figure 1: A healthy intervertebral disc [10]

and not the relative size of the fragments, it is unclear if T1rho relaxation times are sensitive to enzymatic cleavage of the proteoglycans or merely to their total amount. Being able to measure these subtle changes in proteoglycan fragmentation with a technique like T1rho would allow us to better differentiate early stage pathologic disc degeneration from physiologic degeneration.

To clarify these mechanisms, we built and scanned a series of MRI phantoms made to isolate the contributions of proteoglycan concentration and molecular weight on T1rho relaxation times. These phantoms were composed of 2 percent agarose (chosen to mimic physiologic T1rho relaxation values found in the disc) and a proteoglycan stand in. With a similar range of molecular weights and charge per unit mass as native sulfated glycosaminoglycans (the most abundant proteoglycan in the disc), dextran sodium sulfate salt was used to represent proteoglycans. We had two sets of phantoms: one set containing dextrans of a single molecular weight per phantom, and a second set containing dextrans with a range of molecular weights per phantom. Our phantoms spanned three different dextran concentrations and molecular weights, which were selected to mirror in vivo proteoglycan concentrations and fragment sizes[11].

2 Methods

2.1 Phantoms with Single Dextran Size

Ten phantoms having different concentrations and molecular weights of dextran were made (**Table 1**). Each 25ml phantom was composed of 2 percent agarose (Fisher Scientific BP160-500) combined with the prescribed concentration and molecular weight of dextran sodium sulfate salt (**Fig. 2**). First, agarose and deionized water were combined in a conical flask and then heated to 95C to melt the agarose. The heated agarose solution was then transferred to a 50ml conical tube and placed in an 80C water bath to prevent gelling. Meanwhile, dextran was solubilized in deionized water on a heated stir plate. The solution was poured into a 15ml falcon tube and then placed in the water bath and heated until the dextran solution reached 80C. Finally, the warmed dextran solution was added to the 50ml agarose solution, gently mixed, and then allowed to gel at room temperature.

2.2 Phantoms with Sonicated Dextran

To create phantoms having a distribution of dextran sizes, we sonicated 500-kDa dextran solutions for increasing amounts of time. This validated method for mechanically degrading large dextrans into smaller fragments was chosen because it allows precise control of the median fragment size. Dextran sulfate sodium salt (500 kDa) was first solubilized in a beaker of dionized water. The beaker was then sonicated at 20kHz, 100W (Fisher Scientific FB7051100) for 5, 20, 40, 60, 90, 120, 150, or 180 minutes. After sonication, the dextran solutions were decanted into individual conical tubes and stored in an

Table 1: Dextran concentration (dry weight) and molecular weight (kDa) for all 10 phantoms

Phantom	Dextran Molecular Weight (kDa)	Dextran/Dry Weight (mg/g)
Agarose Control	X	X
Large Fragment, High Concentration Dextran	500	400
Large Fragment, Medium Concentration Dextran	500	250
Large Fragment, Low Concentration Dextran	500	100
Medium Fragment, High Concentration Dextran	40	400
Medium Fragment, Medium Concentration Dextran	40	250
Medium Fragment, Low Concentration Dextran	40	100
Small Fragment, High Concentration Dextran	8	400
Small Fragment, Medium Concentration Dextran	8	250
Small Fragment, Low Concentration Dextran	8	100



Figure 2: An example of the dextran, agarose gel phantom



Figure 3: Custom foam phantom holder

80C water bath before being combined with 2 percent liquid agarose as described above. To convert sonication time to average dextran molecular weight, we used previously reported relationships from the literature [12] [13].

2.3 T1rho/T2 Weighted MRI Sequence

All MRI scanning was conducted on a GE 3T Scanner. A combined T1rho/T2 MAPSS sequence was used [14]. For the T1rho acquisition, we used two spinlock frequencies (300Hz and 500Hz) with spin lock times at 0ms, 10ms, 40ms, and 80ms. Scans were acquired coronally with a 20-cm x 20-cm x 0.72-cm field of view with a spatial resolution of 0.4-mm (18 slices total). The conical tubes were secured in a custom foam holder that was placed in the center of the MRI bed (**Fig. 3**).

2.4 Images Processing

The MRI scan data were saved in DICOM format and processed using Matlab. Each conical tube was masked with a 12-pixel radius circular region-of-interest (**ROI; Fig. 4**). The central seven slices of each conical tube ROI was used for data analysis. Specifically, we calculated the T1rho relaxation time on a voxel-by-voxel basis by fitting the signal intensity (SI) to the mono-exponential decay function:

$$SI = S_0 e^{(-TSL/T1rho)} \quad (1)$$

where TSL is the spinlock time.

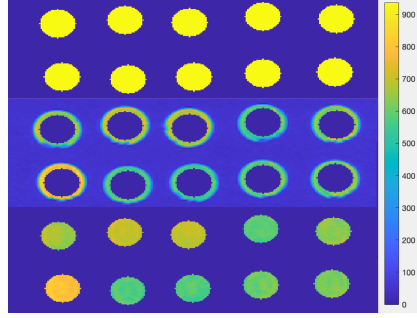


Figure 4: Top: circular ROIs were used to mask the central region of each conical tube. Middle: masked conical tubes showing the central region of each tube for mean T1rho calculation. Bottom: Final ROIs for T1rho analysis. Legend=signal intensity

Table 2: Effects of dextran size on mean T1rho relaxation time for 500 Hz spinlock time. Data given as mean \pm SD

MW Concentration	500kDa	40kDa	8kDa	ANOVA
100mg/g	55.7 \pm 1.6ms	64.3 \pm 1.7ms ^{a,c}	63.5 \pm 1.7ms ^{b,c}	p<.0001
250mg/g	58.2 \pm 1.6ms	62.3 \pm 1.6ms ^a	63.3 \pm 1.6ms ^b	p<.0001
400mg/g	58.1 \pm 1.2ms	62.8 \pm 1.8ms ^{a,c}	58.8 \pm 1.4ms ^c	p<.0001

a: p<.05 500kDa vs 40kDa b: p<.05 500kDa vs 8kDa c: p<.05 40kDa vs 8kDa

2.5 Data Analysis

All statistical tests were conducted using seven axial slice-wise mean T1rho relaxation times for each phantom. Three one-way ANOVA with Turkey HSD tests were performed to determine the effects on T1rho relaxation time of dextran size for each concentration. Anderson Darling tests were used to check the normality of the axial slice-wise mean T1rho values for each phantom.

3 Results

3.1 Phantoms with Single Dextran Size

Phantoms with the largest molecular weight dextran (500 kDa) had significantly ($p < .05$) lower T1rho relaxation times than phantoms with smaller dextrans (**Table 2, Fig. 5**). Dextran concentration appeared to have opposite effects on T1rho relaxation time for the smallest and largest molecular weights. Specifically, for the phantoms with the largest dextran (500 kDa), increasing dextran concentration tended to increase the T1rho relaxation time, whereas for the phantoms with the smallest dextran (8 kDa), increasing dextran concentration decreased the T1rho relaxation time.

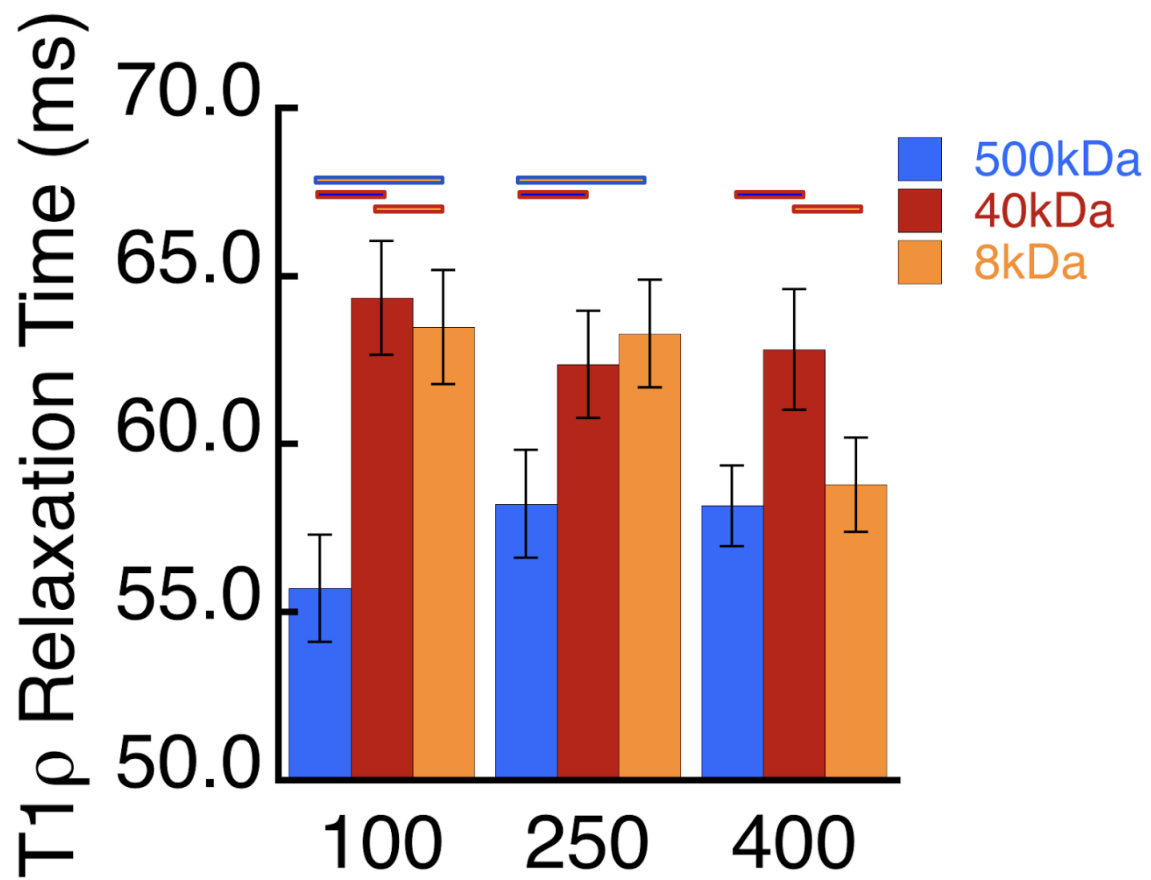


Figure 5: Column chart of mean T1ρ relaxation time(ms) at 500Hz spinlock sequence with STD. Lines across top indicate statistically significant ($p < .05$) differences.

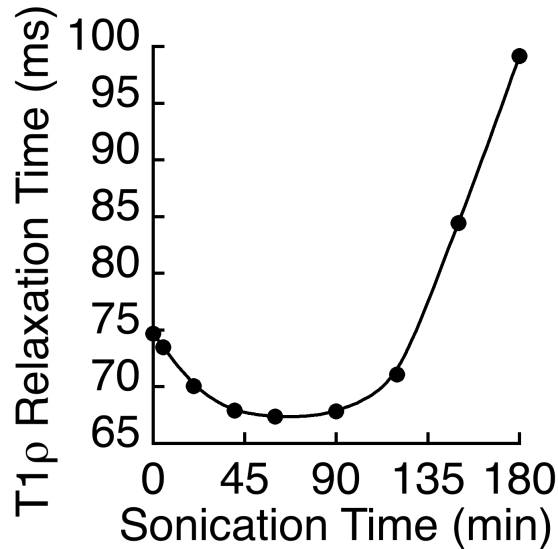


Figure 6: Effects of dextran size and concentration on T1rho relaxation time(ms) at 500Hz spinlock frequency. Bars show mean \pm SD.

3.2 Phantoms with Sonicated Dextran

Increasing the sonication time significantly decreased the mean T1rho time for sonication times (< 60) minutes; for sonication times (> 60) minutes, T1rho relaxation times rapidly increased (**Fig. 6**).

When sonication times were converted to average molecular weight, the decreasing T1rho relaxation times appear to reach an inflection point and begin to rapidly increase when the size of the dextran falls below 50 kDa (**Fig. 7**).

4 Discussion

In this study, we investigated how polysaccharide size affected T1rho relaxation time for various concentrations. Utilizing agarose MRI phantoms containing dextrans with a single molecular weight, we found that the effect of increasing polysaccharide concentration on T1rho relaxation time depended on molecular weight: increasing the concentration of larger dextrans increased the T1rho relaxation time, whereas increasing the concentration of smaller dextrans decreased T1rho relaxation time. Utilizing phantoms with a gradient of molecular weights, we again saw a size-dependent relationship between increased mechanical degradation and T1rho relaxation times. By discovering these new, size-dependent trends, we are able to better understand and interpret findings from studies that measured T1rho relaxation times in patients [15]. Proteoglycan fragmentation is an early marker of disc degeneration that precedes proteoglycan loss from the disc. Prior studies reported that T1rho relaxation times are correlated with disc proteoglycan content. Thus, our findings are important because they are the first to show that T1rho relaxation times are also sensitive to polysaccharide fragment size, and therefore T1rho relaxation times in the disc may reflect proteoglycan degradation in the very early stages of disc degeneration.

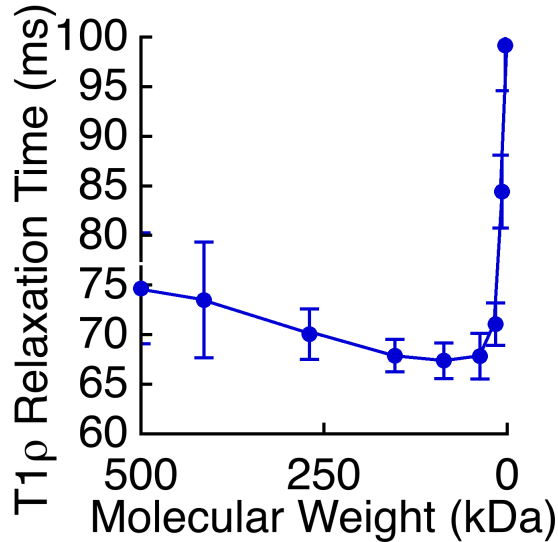


Figure 7: Effects of sonication time on T1rho relaxation time at 300Hz spinlock

In phantoms containing dextrans of a single molecular weight, we found that both dextran molecular weight and concentration had statistically significant effects on T1rho relaxation times. However, the larger dextrans behaved differently than the smaller molecular weight dextrans in regard to the change in T1rho relaxation time with decreasing concentration. Our findings with the large 500-kDa dextran corroborate results from prior studies that showed that T1rho values are lower in discs with less glycosaminoglycan content[16]. However, for the smaller 40kDa and 8kDa dextrans, lower concentrations had greater T1rho relaxation times. We hypothesize that at higher concentrations, phantoms with smaller fragments are more likely to have dextran-dextran interactions than phantoms with larger fragments because there is a significantly higher quantity of these low molecular weight fragments. Since the 500kDa dextran mimics the most physiologically abundant matrix proteins found in the NP, this may explain why our results more closely follow the reported relationships between T1rho and proteoglycan content from human disc studies in the literature. It is unclear if the observed trend of increasing concentration of 8kDa and 40kDa dextran leading to lower T1rho relaxation times has physiologic relevance in human discs.

Another important finding is that mechanical fragmentation of dextran lowered the T1rho relaxation time when the dextran fragments were relatively large, but that fragmentation increased the T1rho relaxation time after the fragments reached 50kDa. For short sonication times (< 60) minutes), mechanical fragmentation of the large 500-kDa dextran are expected to reduce the T1rho relaxation time, as the decrease in concentration of 500kDa dextran is thought to be the main driver. After 60-90 minutes of sonication, however, we propose the dominant mechanism affecting T1rho relaxation transitions from the large dextran fragments to the increasingly numerous smaller dextran fragments, which we have observed to cause a higher T1rho value. Converting sonication time into molecular weight,

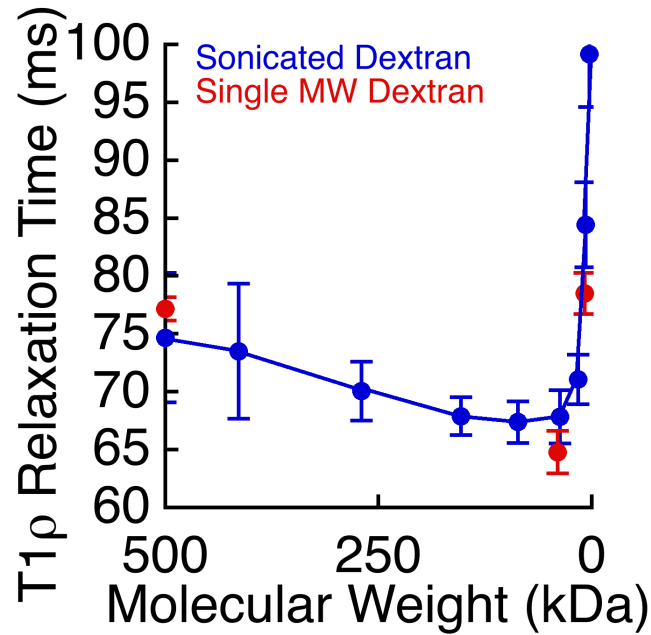


Figure 8: T1rho relaxation time at 300Hz spinlock (ms) vs molecular weight kDa for sonicated dextran (blue) and the single molecular weight dextran phantoms (red) with STD

the transition appears to occur when the average molecular weight is about 50kDa. Adding the T1rho relaxation times from phantoms containing dextrans with a single, known molecular weight, revealed similar T1rho relaxation times for both the sonicated and single molecular weight phantoms, which supports the validity of this interpolation (**Fig. 8**).

The trend observed in the sonication phantoms of this study corroborate the changes in T1rho relaxation time measured in an enzymatically induced degeneration bovine model from our lab. In that study, bovine discs were treated intradiscally with PBS and the aggrecanase ADAMTS-5. ADAMTS-5 cleaves aggrecan (250kDa) into a 200kDa and 50kDa fragment [17]. In that bovine study, discs treated with the highest dose of ADAMTS-5 had a 6ms decrease in mean T1rho relaxation time, which suggests that aggrecan fragmentation decreases T1rho relaxation time. In support of this interpretation, T1rho relaxation times decreased by 5ms, on average, when comparing phantoms with sonicated dextrans in the 250kDa and 50kDa ranges (**Fig 9**).

A strength of our study was the incorporation of specific dextrans in the agarose phantoms to mimic physiologic proteoglycan compositions. Dextrans have a similar charge per unit mass, and the range of dextran concentrations and sizes that we used match those found in vivo. Accordingly, measured T1rho relaxation times were similar to the range of T1rho values observed in clinical cohorts [15]. In addition, we used sonication to mechanically degrade large dextrans into smaller fragments, which may provide mechanistic insight into the effects of early-stage disc degeneration on T1rho values.

However, considering that proteoglycans are not the only molecules in the disc, the phantoms were a simplification of disc biology. Lacking components like collagen, fibronectin, and cartilage, further work

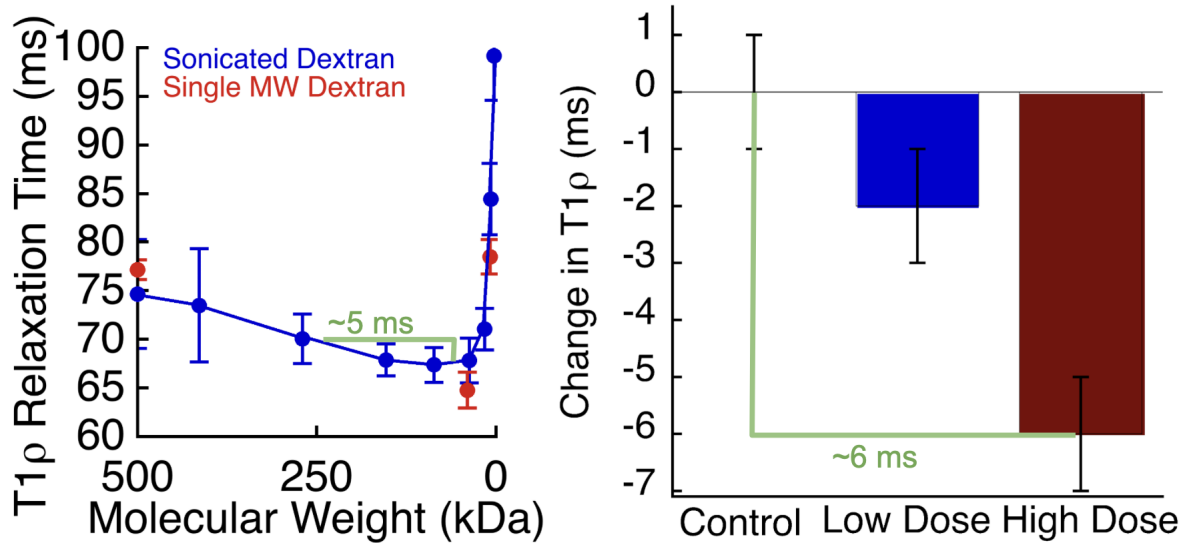


Figure 9: (Left) T1rho relaxation time vs. molecular weight data showed that phantom solutions with 50kDa dextrans are expected to have T1rho relaxation times that are ~5ms lower than phantoms with 250kDa dextran. (Right) Change in T1rho relaxation time following intradiscal ADAMTS-5 treatment in bovine coccygeal discs

needs to be done to clarify the specific factors that affect T1rho with degeneration in vivo. Another limitation of this study is that we did not measure dextran molecular weight following sonication. Although the phantoms with dextrans of known molecular weight had T1rho values that were similar to the T1rho values as the phantoms with estimated molecular weights from the literature, the precise distribution of dextran sizes at each time point is unknown.

5 Conclusion

T1rho-weighted MRI is promising as a noninvasive, quantitative, and highly sensitive biomarker of early-stage disc degeneration. To clarify the factors that impact T1rho relaxation time, we employed agarose phantoms with known concentrations and sizes of polysaccharide dextran. Our findings show for the first time that T1rho relaxation times are sensitive to polysaccharide fragment size, and therefore, T1rho relaxation times in the disc may reflect proteoglycan degradation in the very early stages of disc degeneration..

References

- [1] Erwin, W. M., Hood, K. E. (2014). The cellular and molecular biology of the intervertebral disc: A clinician's primer. *The Journal of the Canadian Chiropractic Association*, 58(3), 246–257.
- [2] Adams MA, Roughley PJ. What is intervertebral disc degeneration, and what causes it? *Spine (Phila Pa 1976)*. 2006 Aug 15;31(18):2151-61. doi:10.1097/01.brs.0000231761.73859.2c. PMID: 16915105.
- [3] Moon, S. M., Yoder, J. H., Wright, A. C., Smith, L. J., Vresilovic, E. J., Elliott, D. M. (2013). Evaluation of intervertebral disc cartilaginous endplate structure using magnetic resonance imaging. *European spine journal : official publication of the European Spine Society, the European Spinal Deformity Society, and the European Section of the Cervical Spine Research Society*, 22(8), 1820–1828. <https://doi.org/10.1007/s00586-013-2798-1>
- [4] Medical Advisory Secretariat (2006). Artificial discs for lumbar and cervical degenerative disc disease -update: an evidence-based analysis. *Ontario health technology assessment series*, 6(10), 1–98. 6. Hong, C., Lee, C. G., Song, H. (2021). Characteristics of lumbar disc degeneration and risk factors for collapsed lumbar disc in Korean farmers and fishers. *Annals of occupational and environmental medicine*, 33, e16.
- [5] Khan AN, Jacobsen HE, Khan J, Filippi CG, Levine M, Lehman RA Jr, Riew KD, Lenke LG, Chahine NO. Inflammatory biomarkers of low back pain and disc degeneration: a review. *Ann N Y Acad Sci*. 2017 Dec;1410(1):68-84. doi: 10.1111/nyas.13551. PMID: 29265416; PMCID: PMC5744892.
- [6] Empere M, Wang X, Prein C, Aspberg A, Moser M, Oohashi T, Clausen-Schaumann H, Aszodi A, Alberton P. Aggrecan governs intervertebral discs development by providing critical mechanical cues of the extracellular matrix. *Front Bioeng Biotechnol*. 2023 Mar 2;11:1128587. doi: 10.3389/fbioe.2023.1128587. PMID: 36937743; PMCID: PMC10017878.
- [7] Roughley PJ, Melching LI, Heathfield TF, Pearce RH, Mort JS. The structure and degradation of aggrecan in human intervertebral disc. *Eur Spine J*. 2006 Aug;15 Suppl 3(Suppl 3):S326-32. doi: 10.1007/s00586-006-0127-7. Epub 2006 May 31. PMID: 16736203; PMCID: PMC2335376.
- [8] Wáng YX, Zhang Q, Li X, Chen W, Ahuja A, Yuan J. T1 magnetic resonance: basic physics principles and applications in knee and intervertebral disc imaging. *Quant Imaging Med Surg*. 2015 Dec;5(6):858-85. doi: 10.3978/j.issn.2223-4292.2015.12.06. PMID: 26807369; PMCID: PMC4700236.
- [9] Borthakur A, Maurer PM, Fenty M, Wang C, Berger R, Yoder J, Balderston RA, Elliott DM. T1 magnetic resonance imaging and discography pressure as novel biomarkers for

- disc degeneration and low back pain. *Spine (Phila Pa 1976)*. 2011 Dec 1;36(25):2190-6. doi: 10.1097/BRS.0b013e31820287bf. PMID: 21358489; PMCID: PMC4002043.
- [10] "File:716 Intervertebral Disk.svg." Wikimedia Commons. 3 Jun 2023, 11:01 UTC. 29 May 2024, 20:08
- [11] Iatridis JC, MacLean JJ, O'Brien M, Stokes IA. Measurements of proteoglycan and water content distribution in human lumbar intervertebral discs. *Spine (Phila Pa 1976)*. 2007 Jun 15;32(14):1493-7. doi: 10.1097/BRS.0b013e318067dd3f. PMID: 17572617; PMCID: PMC3466481.
- [12] Ohta, Kazuko, et al. "Ultrasonic Degradation of Dextran in Solution." *Kobunshi Ronbunshu*, vol. 40, no. 7, 1983. 417.
- [13] Qingsong Zou, Yuanyuan Pu, Zhong Han, Nan Fu, Suxia Li, Mei Liu, Lei Huang, Angen Lu, Jianguang Mo, Shan Chen, Ultrasonic degradation of aqueous dextran: Effect of initial molecular weight and concentration, *Carbohydrate Polymers*, Volume 90, Issue 1, 2012, Pages 447-451, ISSN 0144-8617, <https://doi.org/10.1016/j.carbpol.2012.05.064>.
- [14] Li, X., Han, E.T., Busse, R.F. and Majumdar, S. (2008), In vivo T1 mapping in cartilage using 3D magnetization-prepared angle-modulated partitioned k-space spoiled gradient echo snapshots (3D MAPSS). *Magn. Reson. Med.*, 59: 298-307. <https://doi.org/10.1002/mrm.21414>
- [15] Bonnheim NB, Lazar AA, Kumar A, Akkaya Z, Zhou J, Guo X, O'Neill C, Link TM, Lotz JC, Krug R, Fields AJ. ISSLS Prize in Bioengineering Science 2023: Age- and sex-related differences in lumbar intervertebral disc degeneration between patients with chronic low back pain and asymptomatic controls. *Eur Spine J*. 2023 May;32(5):1517-1524. doi: 10.1007/s00586-023-07542-6. Epub 2023 Feb 18. PMID: 36805320; PMCID: PMC10205694.
- [16] Johannessen W, Auerbach JD, Wheaton AJ, Kurji A, Borthakur A, Reddy R, Elliott DM. Assessment of human disc degeneration and proteoglycan content using T1rho-weighted magnetic resonance imaging. *Spine (Phila Pa 1976)*. 2006 May 15;31(11):1253-7. doi: 10.1097/01.brs.0000217708.54880.51. PMID: 16688040; PMCID: PMC2855820.
- [17] "Human Aggrecan (ADAMTS5-Cleaved) Antibody." [Www.Rndsystems.Com](http://www.rndsystems.com), www.rndsystems.com/products/human-aggrecan-adamts5-cleaved-antibody-726006_mab64891. Accessed 19 Aug. 2024.

Publishing Agreement

It is the policy of the University to encourage open access and broad distribution of all theses, dissertations, and manuscripts. The Graduate Division will facilitate the distribution of UCSF theses, dissertations, and manuscripts to the UCSF Library for open access and distribution. UCSF will make such theses, dissertations, and manuscripts accessible to the public and will take reasonable steps to preserve these works in perpetuity.

I hereby grant the non-exclusive, perpetual right to The Regents of the University of California to reproduce, publicly display, distribute, preserve, and publish copies of my thesis, dissertation, or manuscript in any form or media, now existing or later derived, including access online for teaching, research, and public service purposes.

DocuSigned by:

Joanna Veres

504CC3C673B3469...

Author Signature

8/30/2024

Date